

## Ordered and disordered phospholipid domains coexist in membranes containing the calcium pump protein of sarcoplasmic reticulum

(1,6-diphenyl-1,3,5-hexatriene/protein-lipid interactions/ $\text{Ca}^{2+}$ -ATPase/differential scanning calorimetry/membrane ultrastructure)

BARRY R. LENTZ, KENNETH W. CLUBB, DAVID A. BARROW, AND GERHARD MEISSNER

Department of Biochemistry and Nutrition, University of North Carolina, Chapel Hill, North Carolina 27514

Communicated by Carl W. Gottschalk, February 10, 1983

**ABSTRACT** Data are presented that lead to an alternative model for the organization and molecular dynamics of lipid molecules near the  $\text{Ca}^{2+}$ -stimulated,  $\text{Mg}^{2+}$ -dependent adenosinetriphosphatase ( $\text{Ca}^{2+}$ -ATPase; ATP phosphohydrolase, EC 3.6.1.3) of sarcoplasmic reticulum. Measurements of the steady-state fluorescence anisotropy of 1,6-diphenyl-1,3,5-hexatriene in progressively delipidated sarcoplasmic reticulum membranes have been quantitatively interpreted in terms of a layer of lipid of high anisotropy (the lipid annulus) coexisting with lipid layers of very low anisotropy. In addition, the  $\text{Ca}^{2+}$ -ATPase has been reconstituted into pure 1,2-dipentadecanoyl 3-*sn*-phosphatidylcholine membranes over a range of lipid-to-protein ratios. High-sensitivity differential scanning calorimetry has demonstrated that roughly 30 lipid molecules per  $\text{Ca}^{2+}$ -ATPase molecule (annular lipids) fail to undergo a calorimetrically detectable phase transition in the temperature range 4–44°C. Roughly 100 lipid molecules beyond the annulus undergo a detectable phase transition at a temperature below the phase transition of pure lipid and with an enthalpy change [4.2 kcal/mol (1 kcal = 4.18 kJ)] about half that observed for pure lipid vesicles (7.7–7.8 kcal/mol). We propose that both the fluorometric and calorimetric data are consistent with a model in which a motionally inhibited lipid annulus is surrounded by a more extensive region of disrupted lipid packing order, which we have called the secondary lipid domain.

The effect of an intrinsic membrane protein on the molecular structure and dynamics of its surrounding lipid bilayer has been the subject of intense debate in recent years. Mainly on the basis of ESR and fluorescent probe studies, it is widely believed that proteins inserted into the membrane tend to restrict the motion of neighboring lipid molecules (see refs. 1 and 2 for reviews). These studies have suggested the coexistence of normal and motionally restricted bilayer domains within protein-containing membranes (3–5). The restricted, protein-associated domain is frequently referred to as “annular” (5) or “boundary” (3) lipid. However, there is not universal agreement with this view. The major objection to this simple model has been that deuterium nuclear magnetic resonance ( $^2\text{H}$  NMR) probes display a spectrum characteristic of a more disordered environment in protein-lipid recombinant membranes than in pure lipid bilayers (6, 7). A possible resolution of the apparent disparity between ESR and  $^2\text{H}$  NMR has been suggested in terms of both the different time resolutions of these two techniques and a proposed disordered protein surface (6, 8). Other objections to the boundary model have stressed protein aggregation as a possible source of “trapped” and therefore motionally inhibited lipid (9, 10) or the fact that quantitative data analysis suggests the presence of more than just boundary and normal

lipids in membranes containing intrinsic proteins (11–13).

In this communication, we present evidence for a model of protein-lipid interactions in which a domain of disrupted lipid order coexists with a domain of enhanced order, presumed to be the boundary domain. This model offers a resolution of the conflicting viewpoints derived from ESR and  $^2\text{H}$  NMR results and makes predictions that provide an explanation for the permeability properties of biomembranes. Preliminary data in support of this model have been presented (14).

### MATERIALS AND METHODS

Microsomes containing the  $\text{Mg}^{2+}$ -dependent,  $\text{Ca}^{2+}$ -stimulated adenosinetriphosphatase ( $\text{Ca}^{2+}$ -ATPase; ATP phosphohydrolase, EC 3.6.1.3) were isolated from rabbit white muscle and delipidated with sodium cholate as described (13), resulting in membranes containing endogenous phospholipid at various lipid-to-protein ratios, and in which the protein content was 90%  $\text{Ca}^{2+}$ -ATPase. These were used in our fluorometric studies. For calorimetric studies, such membrane preparations were further delipidated by precipitation with polyethylene glycol and remaining native lipids were replaced by synthetic 1,2-dipentadecanoyl 3-*sn*-phosphatidylcholine [( $\text{C}_{15}$ )<sub>2</sub>-PtdCho; Avanti Biochemicals] in the presence of sodium deoxycholate, using procedures similar to those previously described (15). The only modification was removal of solubilizing detergent by dialysis for 48–72 hr at the lipid pretransition temperature (22°C), followed by incubation of the reconstituted membranes for 3 hr at 38°C. Freeze-fracture electron micrographs, prepared by jet-freezing (15), revealed membranous morphology, although closed vesicles were not always observed, especially for samples with very high or very low lipid-to-protein ratios. Membrane morphology remained unchanged for months in frozen samples stored at –70°C and was unaffected by storage above the lipid phase transition for several hours. Less than 1 mol % native lipid could be detected in the replaced membranes by gas chromatographic analysis (15). Contamination by residual deoxycholate was always less than could be detected by [ $^{14}\text{C}$ ]deoxycholate radioactivity (usually  $\leq 0.01$  mol per mol of  $\text{Ca}^{2+}$ -ATPase). After solubilization in dodecyltetraoxyethylene glycol monoether (16), all native-lipid and lipid-replaced samples showed 80–100% native  $\text{Ca}^{2+}$ -ATPase activity (15).

Steady-state measurements of 1,6-diphenyl-1,3,5-hexatriene (DPH) fluorescence anisotropy were made on a Perkin-Elmer MPF-3 spectrofluorometer (17) and were corrected for light-scattering depolarization (18). DPH was incorporated into na-

The publication costs of this article were defrayed in part by page charge payment. This article must therefore be hereby marked “advertisement” in accordance with 18 U.S.C. §1734 solely to indicate this fact.

Abbreviations: SR, sarcoplasmic reticulum;  $\text{Ca}^{2+}$ -ATPase,  $\text{Mg}^{2+}$ -dependent,  $\text{Ca}^{2+}$ -stimulated adenosinetriphosphatase; ( $\text{C}_{15}$ )<sub>2</sub>-PtdCho, 1,2-dipentadecanoyl 3-*sn*-phosphatidylcholine; DPH, 1,6-diphenyl-1,3,5-hexatriene.

tive lipid membranes by injection of a small volume ( $<1 \mu\text{l}$ ) of a tetrahydrofuran solution of DPH at room temperature, followed by incubation at  $4^\circ\text{C}$  overnight. DPH-to-lipid ratios were maintained in the range of 1:300 to 1:500.

Heat capacity profiles were obtained on lipid-replaced membranes by using a high-sensitivity differential scanning calorimeter (Tronac 750) especially built for us by Roger Hart of Hart Scientific (Orem, UT). This calorimeter is a modification of a design used previously by Suurkuusk *et al.* (19) and is highly sensitive to changes in heat capacity, as required to detect the broad and subtle lipid phase transitions reported here.  $\text{Ca}^{2+}$ -ATPase-containing membranes used for calorimetry were suspended in 0.1 M KCl/1 mM  $\text{MgCl}_2$ /0.01 M 2-[tris(hydroxymethyl)methyl]amino]ethanesulfonic acid (Tes) buffer, pH 7.5, containing 20% glycerol, which was essential for maintenance of  $\text{Ca}^{2+}$ -ATPase activity during the 6–8 hr required for heating and subsequent cooling scans at rates of  $\pm 15^\circ\text{C}/\text{hr}$ .

## RESULTS

In Fig. 1, we show the dependence of DPH fluorescence anisotropy on protein and lipid content of native and partially delipidated SR membranes. Earlier, we tested the ability of the boundary lipid model to fit these data, using the assumption of two independent lipid domains (13). One domain was assumed to be a boundary layer containing 34 lipid molecules per protein molecule and displaying the DPH fluorescence anisotropy ( $r_1$ ) of such a sample. The other domain was assumed to display the anisotropy ( $r_2$ ) of multilamellar lipid vesicles containing no protein. With these assumptions, the overall average anisotropy at different temperatures ( $T$ ) and protein mol fractions ( $Y_p$ ) could be calculated as:

$$r(T, Y_p) = Z_1(Y_p) [r_1(T) - r_2(T)] + r_2(T), \quad [1]$$

in which  $Z_1$  is the intensity-weighted mol fraction of DPH lo-

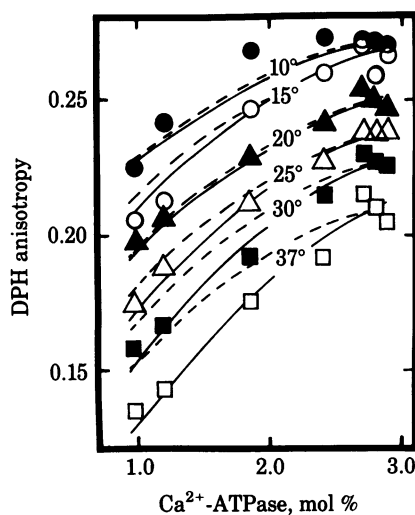


FIG. 1. Dependence of DPH fluorescence anisotropy on  $\text{Ca}^{2+}$ -ATPase content of partially delipidated SR membranes. Data at  $10^\circ$  (●),  $25^\circ$  (Δ), and  $37^\circ\text{C}$  (■) have been reported (13). New data are presented for  $15^\circ$  (○),  $20^\circ$  (▲), and  $30^\circ\text{C}$  (■). Calculated anisotropies (13) are shown for two simple binary-lipid-domain models. In the first model (---), one domain is assumed to be boundary lipid (34 lipid molecules per  $\text{Ca}^{2+}$ -ATPase) and the other to be bulk lipid having properties of multilamellar vesicles containing no protein. In the second model (—), boundary lipid is assumed to be surrounded by a disrupted secondary lipid domain. DPH fluorescence anisotropies ( $r_2$ ) of the secondary lipid domain resulting in the best calculated fit (—) are plotted in Fig. 2 for each of the six temperatures shown here.

cated in the boundary domain. The calculation of  $Z_1$  is detailed in appendix B of ref. 13. The anisotropies calculated according to this *boundary lipid model* are shown by broken curves in Fig. 1. As previously noted (13), the calculated anisotropies failed to reproduce the experimental data above  $20^\circ\text{C}$ . As a possible explanation, we now propose that beyond the annular layer of lipid there is a “secondary” lipid domain having a disrupted packing order relative to that of bulk lipid. Indeed, because of the low lipid-to-protein ratio in native SR membrane (*ca.* 100 lipid molecules per  $\text{Ca}^{2+}$ -ATPase), we suggest, as a first approximation, that this membrane contains no lipid characterized by the anisotropy observed in a protein-free lipid bilayer.

In order to test this *disrupted secondary lipid domain model*, we varied the DPH fluorescence anisotropy assigned to the nonboundary lipid ( $r_2$  in Eq. 1) for each temperature in Fig. 1 so as to obtain the best fit of calculated average anisotropies (Eq. 1) to the observed data (nonlinear least-squares method). At each temperature, this procedure reproduced well the experimental data, as shown by the solid curves of Fig. 1. The  $r_2$  (secondary lipid anisotropy) values generated in this way are plotted in Fig. 2 and turned out to be linearly dependent on temperature. This meant that only a single adjustable parameter ( $dr_2/dT$  in Fig. 2) was required to completely describe the variation of overall DPH fluorescence anisotropy with both temperature and protein content in the SR membrane.

The number of lipids associated with the boundary domain was fixed at 34 lipid molecules per  $\text{Ca}^{2+}$ -ATPase on the basis of previous activity (5) and ESR (4) measurements. More recent ESR spectral analyses have yielded values of approximately 30 (20) or 20–30 (10) lipid molecules per  $\text{Ca}^{2+}$ -ATPase. For this reason, we tested the sensitivity of our calculations to the boundary lipid-to-protein ratio. We found the fit to be essentially unaffected by assuming a lipid-to-protein ratio of 30 instead of 34 (Fig. 2). However, assuming a value of 25 lipid molecules per protein molecule (Fig. 2) resulted in a worse fit (total square deviation was doubled).

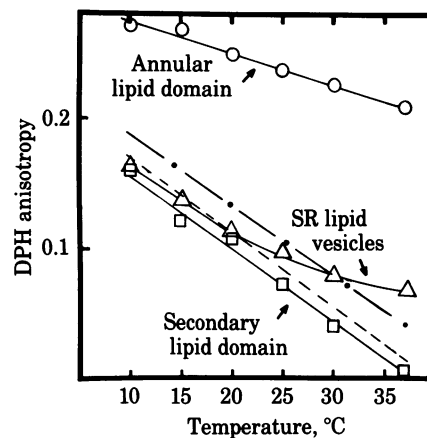


FIG. 2. Temperature dependence of the DPH fluorescence anisotropy presumed to reflect molecular order in annular ( $r_1$ ) and secondary ( $r_2$ ) lipid domains. The anisotropy measured in partially delipidated SR membranes is taken as  $r_1$  for the presumed boundary lipid domain (○). The anisotropy values ( $r_2$ ) associated with the presumed secondary lipid layer (□) are also plotted at the different temperatures for which they were calculated, under the assumption that 34 lipid molecules per protein molecule existed in the annular lipid layer. Additional lines show the temperature dependence of the secondary lipid domain DPH fluorescence anisotropy calculated under the assumptions that the annulus contained 30 (---) and 25 (—) lipid molecules per protein. For comparison, data are also presented for multilamellar vesicles prepared from extracted SR lipid (Δ).

The secondary lipid domain model inherently assumes that the principal reason for failure of the simple boundary lipid model is disruption of lipid packing beyond the boundary layer. Variations with protein content in the properties of the motionally inhibited boundary lipid domain have been ignored in this simple model. Nonetheless, such variations in the boundary layer have been suggested on the basis of some ESR studies (9, 20).

To test the ability of a *variable boundary lipid model* to account for our data, we tried to fit our experimental data by varying either the size of the boundary domain,  $\alpha$ , or the fluorescence anisotropy associated with this domain,  $r_1$ , while keeping  $r_2$  fixed at the value observed in a pure lipid bilayer. In both instances, a good fit to experiment was obtained only when different values of either  $\alpha$  or  $r_1$  were assigned for each experimental point shown in Fig. 1. In order to simplify the variable boundary lipid model, we approximated the dependence of  $r_1$  on lipid-to-protein ratio as linear. Even so, a new parameter value was required at every temperature to obtain a fit comparable to that obtained with a single parameter value in our secondary domain model. For this reason, we prefer the simpler secondary domain model as a means of accounting for the variation of DPH fluorescence anisotropy with temperature and lipid/protein composition in delipidated SR membranes. However, we cannot completely rule out the variable boundary model on the basis of our fluorometric data alone.

In addition to inferring the properties of protein-affected native (SR) lipids from DPH fluorescence, we have reconstituted the  $\text{Ca}^{2+}$ -ATPase into a synthetic lipid [( $\text{C}_{15}$ )<sub>2</sub>-PtdCho] so as to use the known phase behavior of this phospholipid as a tool for detecting perturbation of the lipid by the inserted protein. Heat capacity profiles for recombinant membranes at different lipid-to-protein ratios are portrayed in Fig. 3. At an infinite lipid-to-protein ratio [pure ( $\text{C}_{15}$ )<sub>2</sub>-PtdCho in Fig. 3], the phase transition was highly cooperative, as evidenced by the sharpness of

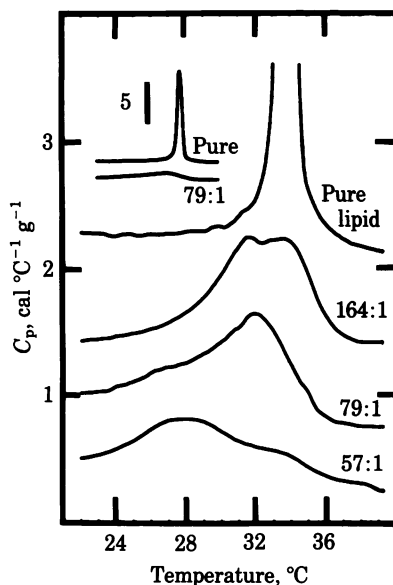


FIG. 3. Temperature dependence of the heat capacity ( $C_p$ ) for membranes containing indicated mol ratios of ( $\text{C}_{15}$ )<sub>2</sub>-PtdCho to  $\text{Ca}^{2+}$ -ATPase (1 cal = 4.18 J). The sample without protein (pure lipid) was prepared by slow dilution and dialysis of an octyl glucoside-solubilized lipid suspension (see text). Data were obtained in cooling scans performed at a rate of  $-15^\circ\text{C}/\text{hr}$  on samples containing 0.5–1.5  $\mu\text{mol}$  of lipid suspended in 0.1–0.2 ml of buffer (see text). (Inset) Relationship of the full pure lipid phase transition to that of the 79:1 sample (note compressed scale). Heat capacity profiles have been shifted vertically for clarity and, therefore, should be interpreted as relative rather than as absolute heat capacity profiles.

the peak in heat capacity (21). Pure lipid heat capacity profiles were obtained on large, unilamellar vesicles prepared by slow octyl glucoside dilution and dialysis (22, 23). Such vesicles are similar in size to the reconstituted  $\text{Ca}^{2+}$ -ATPase vesicles, making it possible to meaningfully compare the heat capacity profiles of protein-free and protein-containing vesicles. Upon incorporation of the  $\text{Ca}^{2+}$ -ATPase, the peak in the heat capacity profile became broadened (i.e., less cooperative) and the heat capacity profile developed shoulders at temperatures just below the pure lipid transition temperature. With decreasing lipid-to-protein ratio, the height of the main peak diminished. At a lipid-to-protein ratio of 164, for example (see Fig. 3), the heat capacity profile displayed a greatly reduced main phase transition peak relative to pure lipid vesicles (33.1–33.2°C) as well as a second peak at about 31.2–31.4°C (Table 1) and a subtle shoulder at 27–29°C (Fig. 3). By a lipid-to-protein ratio of 57, the shoulder at 27–29°C became the major remaining peak (Fig. 3).

For all samples examined, the base line was reached on either side of the peaks by 21.5 and 38.5°C. The heat capacity was integrated between these limits by using a first-order fit to the base line and a discontinuity at the peak (24). The molar enthalpies obtained in this way (Table 1) decreased nonlinearly with reduction in the lipid-to-protein ratio (data not shown). The nonlinear variation of the enthalpy with the ratio of protein to lipid and the appearance of a low-temperature peak disagree with the results of Gómez-Fernández *et al.* (25). A likely reason for this disagreement is that the Perkin–Elmer calorimeter used by Gómez-Fernández *et al.* was simply not sufficiently sensitive, even at their high scan rates, to resolve the subtle heat capacity peaks evident in our data at temperatures just below the pure phospholipid phase transition. Also contrary to the suggestion of Gómez-Fernández *et al.* (24), the phase transitions observed in our reconstituted samples seemed not to reflect changes in membrane lateral organization. Freeze-fracture electron micrographs of our preparations showed a uniform distribution of intramembranous particles, at least for 164 or fewer lipid molecules per protein molecule (unpublished data). In addition, no differences in particle organization were observed on either side of the low-temperature heat capacity peak seen in Fig. 3. Thus, the different peaks observed in our heat capacity profiles (Fig. 3) should reflect transitions in local lipid domains surrounding the  $\text{Ca}^{2+}$ -ATPase rather than formation of protein-rich and lipid-rich patches.

The broad and subtle heat capacity peaks observed for all lipid-to-protein ratios must be due to lipid affected in some way by the presence of the protein. Due to the inhibition of acyl chain motion expected for lipid adjacent to the protein, we rea-

Table 1. Thermal properties of order–disorder phase transition in ( $\text{C}_{15}$ )<sub>2</sub>-PtdCho/ $\text{Ca}^{2+}$ -ATPase reconstituted membranes

Lipid/protein, mol/mol	Temperature(s) of the main transition(s), °C		Transition enthalpy, kcal/mol lipid	
	Cool	Heat	Cool	Heat
$\infty$	33.8	33.6	$7.8 \pm 0.5$	$7.7 \pm 0.5$
164	31.4, 33.2	31.2, 33.1	3.8	3.9
79	31.9	31.7	3.2	2.4
57	28.0	27.5	2.0	1.8
27	—	—	<0.02*	<1.3**

\* Estimated from the base-line noise and the maximal likely range of any transition (12°C).

† The noise in this heating scan was abnormally large, although all heating scans with the 20% glycerol buffer were noisier than cooling scans, presumably due to thermal gradients formed while heating this viscous buffer.

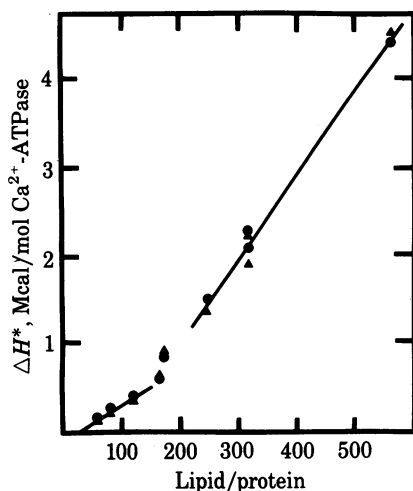


FIG. 4. Dependence of the lipid phase transition enthalpy (between 21.5 and 38.5°C) per mol of  $\text{Ca}^{2+}$ -ATPase ( $\Delta H^*$ ) on the lipid-to-protein ratio in  $(\text{C}_{15})_2$ -PtdCho/ $\text{Ca}^{2+}$ -ATPase reconstituted membranes. Enthalpies were derived from both cooling ( $\bullet$ ) and heating ( $\blacktriangle$ ) scans. Limiting linear fits were obtained by a linear least-squares analysis of the three points at lowest and highest lipid content, as discussed in the text.

soned that annular lipid should not be able to undergo a cooperative phase transition and should display essentially no transition enthalpy. Therefore, the low-temperature peaks should reflect the presence of protein-modified lipid beyond the annular layer. To test this hypothesis, we have plotted in Fig. 4 the phospholipid phase transition enthalpy per mol of  $\text{Ca}^{2+}$ -ATPase as a function of lipid-to-protein ratio. If distinct lipid domains coexist and vary in relative abundance according to the lipid-to-protein ratio, the slope of such a plot should yield the average transition enthalpy of the lipid domain remaining incompletely filled at a given ratio. Thus, at a sufficiently low lipid-to-protein ratio, this slope should yield the transition enthalpy of the protein-affected lipid just beyond the lipid annulus. If the disrupted secondary domain model is correct, this enthalpy should differ from that of a bulk lipid bilayer. In addition, the intercept of such a plot with the abscissa should yield the lipid-to-protein ratio of the annular lipid domain, assuming that the annular lipid phase transition cannot be detected calorimetrically. As seen in Fig. 4, our enthalpy data fit these expectations, having a linear region below 150 lipid molecules per protein molecule with a slope of 4.2 kcal/mol of lipid and an intercept of 29 lipid molecules per protein molecule. Above 200 lipid molecules per protein molecule, the curve was also approximately linear, as would be expected for membranes containing pure lipid domains beyond the protein-affected domains. The slope at high lipid-to-protein ratio was 9.2 kcal/mol of lipid, in reasonable agreement with the directly measured values for pure lipid transition enthalpies given in Table 1, and with enthalpies obtained for multilamellar vesicles composed of  $(\text{C}_{15})_2$ -PtdCho [8.3–8.7 kcal/mol (23)]. To test the idea of a calorimetrically undetectable lipid annulus, we prepared a sample containing only 27 lipid molecules per  $\text{Ca}^{2+}$ -ATPase. Heating and cooling calorimetric scans on this sample revealed no heat capacity peak (Table 1) that could be distinguished from base-line noise (0.3 cal/°C per g heating and 0.004 cal/°C per g cooling).

## DISCUSSION

We have shown that our DPH fluorescence data on partially delipidated SR membranes could be interpreted in terms of a disrupted secondary lipid domain. However, our fluorescence results could not rule out a model postulating a variable annular

domain. On the other hand, our calorimetric results on synthetic lipid membranes clearly favor the proposal that the lipid immediately beyond the primary annular layer is considerably altered in structure by the presence of the  $\text{Ca}^{2+}$ -ATPase. Therefore, the secondary lipid domain model accounts for both our fluorometric and calorimetric data. This secondary lipid domain appears on the basis of our fluorescence results to contain disordered acyl chains relative to a protein-free lipid bilayer, especially at high temperature (see Fig. 2). By contrast, our calorimetric experiments do not sense directly the structure of this region, but rather the nature of the phospholipid phase transition which it undergoes. Nonetheless, the reduced enthalpy, the decreased cooperativity, and the lowered phase transition temperature relative to pure phospholipid membranes suggest that the low-temperature phase is thermodynamically less stable due to disrupted lipid packing caused by the presence of the protein.

Fig. 5 illustrates the proposed variation of packing order with distance from the  $\text{Ca}^{2+}$ -ATPase. The disordered region just beyond the annulus results from the difference in lipid packing between the annular layer and the protein-unaffected bilayer further from the protein-lipid interface. The extent of the disrupted region and the severity of the disorder will depend both on the relative cross-sectional areas of the protein and lipids and on the detailed shape of the protein surface. In addition, the disordered region is not expected to be uniformly disordered or to be unaffected by changes in the lipid-to-protein ratio. Thus, we do not observe a single, well-defined, heat capacity peak for protein-affected lipid at all lipid-to-protein ratios, but rather a broad profile whose peak shifts somewhat for different ratios (Fig. 3). In this sense, the enthalpy calculated from Fig. 4 for the phase transition of the disrupted lipid layer must be considered an average value associated with a range of detailed local lipid structures.

We now comment on the relationship between our results and previous literature reports. First, with regard to the lipid disorder reported by  $^2\text{H}$  NMR (6), the secondary lipid region should contain a variety of different lattice sites, many of which should allow substantial reorientation of lipid chains. On the time scale of  $^2\text{H}$  NMR, a probe molecule experiences restricted motion at annular lipid sites as well as substantially unrestricted motion at many sites in the disrupted, secondary-lipid domain.

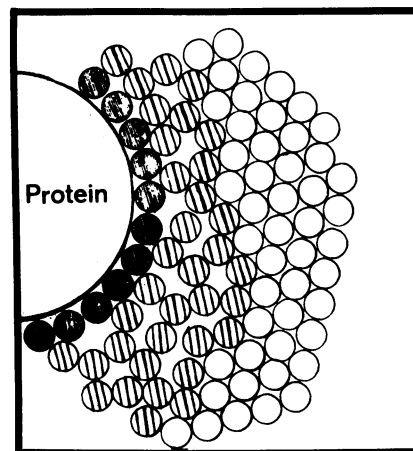


FIG. 5. Proposed model for the primary or boundary (shaded), and disordered or secondary (striped) lipid domains surrounding the  $\text{Ca}^{2+}$ -ATPase in SR membrane. A surface view of the membrane is shown. At a distance sufficiently removed from the protein surface, a lipid domain with the packing order of pure lipid bilayer (unshaded) is presumed, although the pure lipid bilayer domain is likely not present at physiological lipid-to-protein ratios of about 100:1.

Because the motion of the probe is summed over all sites, it appears by  $^2\text{H}$  NMR that the probe has the freedom to reorient through a large angle. This orientational angle-weighted average emphasizes large angular fluctuations and, therefore, the disordered layer. Thus, it is not surprising that  $^2\text{H}$  NMR probes report greater motional freedom in the presence of the  $\text{Ca}^{2+}$ -ATPase relative to a protein-free bilayer. Due to the shorter time scales of fluorescence or ESR experiments, however, such probe molecules report the orientational order reflecting roughly a single lipid lattice site (8). For ESR probes, this results in a composite spectrum reflecting both the annular and secondary lipid environments, whereas, for our DPH fluorescence results, the average order parameter reported is the number average over individual sites. We propose that deconvolution of this average reveals a disordered secondary lipid domain coexisting with an ordered annulus, consistent with both  $^2\text{H}$  NMR and ESR results.

Second, support for the proposed model of coexisting ordered and disordered lipid domains also derives from recent  $^2\text{H}$  NMR results of Seelig *et al.* (26), who analyzed  $T_1$  relaxation times to detect a 20% slowing of segmental reorientation in the presence of the  $\text{Ca}^{2+}$ -ATPase (restricted motion of the annular lipid) along with a decrease in the deuterium order parameter (packing disorder in the secondary lipid layer). In this regard, a recent ESR spectral subtraction study has interpreted a small decrease in hyperfine splitting of the rapid motion component relative to pure lipid as probably reflecting "a small increase in the motion and/or disorder of the bulk phospholipid in the presence of calcium pump protein" (20). Nonetheless, the overall spectrum still showed a significantly broadened component consistent with an immobilized boundary layer (20). In the same vein, recent Fourier transform infrared spectroscopic data have been interpreted as reflecting imperfect lipid packing in the presence of the protein even when the lipid acyl chains are in an ordered configuration (27). These results are consistent with our model but would be difficult to interpret in terms of a boundary layer coexisting with unperturbed bulk lipid.

In fairness, we must note that some ESR spectral subtraction studies of cytochrome oxidase recombinant membranes (28) or delipidated/lipid-replaced SR membranes (10) have concluded that lipids just beyond the lipid annulus are more restricted in their motion than bulk lipid. This is in opposition to the model reported here and apparently also to the ESR,  $^2\text{H}$  NMR, and infrared spectral data discussed above. This conclusion essentially rested on the observation of a slightly broader spectral line, relative to a pure lipid spectrum, in the resolved secondary lipid spectrum after subtraction of a delipidated membrane spectrum. This could result from slower or restricted probe motion or from heterogeneity of probe binding sites in the secondary lipid domain. Our model suggests disrupted lipid packing, but does not address the possibility of slower probe (and consequently acyl chain) motion. However, our model implies site heterogeneity and is, therefore, consistent with one possible interpretation of the ESR results quoted (10, 28).

Finally, analysis of the noise associated with ionic conductance through black lipid membranes has led to the suggestion that proteins may induce bilayer fluctuations that increase the probability of individual ionic permeation events (\*). This would

be consistent with the existence of a disrupted lipid domain with increased permeability beyond the ordered or annular domain directly surrounding an intrinsic membrane protein.

D.A.B. wishes to mark the retirement (August 1982) of his mother, Professor Emily S. Barrow, from the University of North Carolina Department of Pathology, with thanks for her encouragement and inspiration in his pursuit of a career in science. This work was supported by an American Heart Association Grant-in-Aid (81-698) and by grants from the National Science Foundation (PCM79-22733) and U.S. Public Health Service (AM18687). B.R.L. is recipient of an Established Investigator Award of the American Heart Association with partial funds provided by the North Carolina Heart Association.

1. Jost, P. C. & Griffith, O. H. (1980) *Pharm. Biochem. Behav.* **13**, 155-165.
2. Chapman, D., Gómez-Fernandez, J. C. & Goñi, F. M. (1979) *FEBS Lett.* **98**, 211-223.
3. Jost, P. C., Capaldi, R. A., Vanderkooi, G. & Griffith, O. H. (1973) *J. Supramol. Struct.* **1**, 269-280.
4. Nakamura, M. & Onishi, S. (1975) *J. Biochem. (Tokyo)* **78**, 1039-1045.
5. Hesketh, T. R., Smith, G. A., Houslay, M. D., McGill, K. A., Birdsall, N. J. M., Metcalfe, J. C. & Warren, G. B. (1976) *Biochemistry* **15**, 4145-4151.
6. Rice, D. M., Meadows, M. D., Scheinman, A. O., Goñi, F. M., Gómez-Fernandez, J. C., Moscarello, M. A., Chapman, D. & Oldfield, E. (1979) *Biochemistry* **18**, 5893-5902.
7. Paddy, M. R., Dahlquist, F. W., Davis, J. H. & Bloom, M. (1981) *Biochemistry* **20**, 3152-3162.
8. Jähnig, F. (1979) *Proc. Natl. Acad. Sci. USA* **76**, 6361-6365.
9. Davoust, J., Bienvenue, A., Fellmann, P. & Devaux, P. F. (1980) *Biochim. Biophys. Acta* **596**, 28-42.
10. Thomas, D. D., Bigelow, D. J., Squier, T. C. & Hidalgo, C. (1982) *Biophys. J.* **37**, 217-225.
11. Knowles, P. F., Watts, A. & Marsh, D. (1981) *Biochemistry* **20**, 5888-5894.
12. Watts, A., Davoust, J., Marsh, D. & Devaux, P. F. (1981) *Biochim. Biophys. Acta* **643**, 673-676.
13. Moore, B. M., Lentz, B. R. & Meissner, G. (1978) *Biochemistry* **17**, 5248-5255.
14. Lentz, B. R., Moore, B. M., Kirkman, C. & Meissner, G. (1982) *Biophys. J.* **37**, 30-32.
15. Moore, B. M., Lentz, B. R., Hoechli, M. & Meissner, G. (1981) *Biochemistry* **20**, 6810-6817.
16. Dean, W. L. & Tanford, C. (1978) *Biochemistry* **17**, 1683-1690.
17. Lentz, B. R., Friere, E. & Biltonen, R. L. (1978) *Biochemistry* **17**, 4475-4480.
18. Lentz, B. R., Moore, B. M. & Barrow, D. A. (1979) *Biophys. J.* **25**, 489-494.
19. Suurkuusk, J., Lentz, B. R., Barenholz, Y., Biltonen, R. L. & Thompson, T. E. (1976) *Biochemistry* **15**, 1393-1401.
20. McIntyre, J. O., Samson, P., Brenner, S. L., Dalton, L. & Fleischer, S. (1982) *Biophys. J.* **37**, 53-56.
21. Hinz, H.-J. & Sturtevant, J. M. (1972) *J. Biol. Chem.* **247**, 6071-6075.
22. Mimms, L. T., Zampighi, G., Nozaki, Y., Tanford, C. & Reynolds, J. A. (1981) *Biochemistry* **20**, 833-840.
23. Parente, R. A. & Lentz, B. R. (1983) *Biochemistry* **22**, in press.
24. Krishnan, K. S. & Brandts, J. F. (1978) *Methods Enzymol.* **49**, 369-418.
25. Gómez-Fernandez, J. C., Goñi, F. M., Bach, D., Restall, C. J. & Chapman, D. (1980) *Biochim. Biophys. Acta* **598**, 502-516.
26. Seelig, J., Tamm, L., Hymel, L. & Fleischer, S. (1981) *Biochemistry* **20**, 3922-3932.
27. Mendelsohn, R., Dluhy, R., Tarsch, T., Cameron, D. G. & Mantsch, H. H. (1981) *Biochemistry* **20**, 6699-6706.
28. Knowles, P. F., Watts, A. & Marsh, D. (1979) *Biochemistry* **18**, 4480-4487.

\* Kolb, H.-A., Sixth International Biophysical Congress, September 3-9, 1978, Kyoto, Japan, p. 211 (abstr.).